Using Wavelet Transforms for ECG Characterization

An On-line Digital Signal Processing System

J.S. Sahambi[1], S.N. Tandon[2], R.K.P. Bhatt[1]
[1]Electrical Engineering Department; [2]Centre for Biomedical EngineeringIndian Institute of Technology Delhi

The rapid and objective measurement of timing intervals of the electrocardiogram (ECG) by automated systems is superior to the subjective assessment of ECG morphology. The timing interval measurements are usually made from the onset to the termination of any component of the ECG, after accurate detection of the QRS complex. This article describes a real-time system that uses wavelet transforms to overcome the limitations of other methods of detecting QRS and the onsets and offsets of P- and T-waves. Wavelet transformation is briefly discussed, and detection methods and hardware and software aspects of the system are presented, as well as experimental results.

Overview

Previous approaches reported for QRS detection include nonlinear filtering with thresholding [1], artificial intelligence using hidden Markov models [2], and time-recursive prediction techniques [3]. Nonlinear filtering is a common approach to detect QRS complexes [1], but, although it takes considerably less time and is easily implemented, the main drawback of these algorithms is that frequency variation in QRS complexes adversely affects their performance. The frequency band of QRS complexes generally overlaps the frequency band of noise, resulting in both false positives and false negatives. Methods using artificial intelligence are time consuming due to the use of grammar and inference rules. The hidden Markov model approach requires considerable time [2], even with the use of efficient algorithms.

Wavelet analysis is a very promising mathematical tool that gives good estimation of time and frequency localization. Analysis of the signal at various resolutions is accomplished by decomposition into elementary functions that are well localized both in time and frequency domains. The present approach uses a dyadic wavelet to characterize the ECG signal, but the amount of computations needed to implement this technique is quite large, and general-purpose computers alone are not fast enough for on-line implementation. Computational speed can be increased by using digital signal processing (DSP) add-on cards tailor made for such applications.

To evaluate a QRS detector and measurement of timing intervals of the P, the QRS, and the T waves, it is important to use a standard database. There are two such databases available: the MIT BIH database for QRS detection and the CSE ECG Library for timing-interval measurement. The performance of an algorithm with these databases provides a standard means of comparing the basic performance of one algorithm to another.

In this article, the zero crossings of the wavelet transform are used to detect the location of the QRS. QRS width is then determined by locating the onset and offset of the QRS. Once the QRS has been detected, the location, the onsets, offsets, and amplitudes of P and T waves are determined.

Wavelets

Wavelet transformation is a linear operation that decomposes a signal into components that appear at different scales (or resolutions) [4-7]. Let $\Psi(t)$ be a real or complex valued function in $L^2(R)$. The function $\Psi(t)$ is said to be a wavelet if and only if its Fourier transform $\hat{\Psi}(\omega)$ satisfies:

$$\int_{-\infty}^{\infty} \frac{\left|\hat{\Psi}(\omega)\right|^2}{|\omega|} = C_\Psi < \infty \quad (1)$$

This admissibility condition implies that:

$$\int_{-\infty}^{\infty} \Psi(t)dt = 0 \quad (2)$$

which means that $\Psi(t)$ is oscillatory and its area is zero. Let:

$$\Psi_a(t) = \frac{1}{\sqrt{a}}\Psi\left(\frac{t}{a}\right) \quad (3)$$

be the dilation of $\Psi(t)$ by a scale factor of $a > 0$. The factor $\frac{1}{\sqrt{a}}$ in the above expression is used for energy normalization. The wavelet transform of a function $f(t) \epsilon L^2(R)$ at scale a and position τ is given by:

$$Wf(a,\tau) = \frac{1}{\sqrt{a}}\int_{-\infty}^{\infty} f(t)\Psi^*\left(\frac{t-\tau}{a}\right)dt \quad (4)$$

where * denotes the complex conjugation.

This type of transform satisfies energy conservation, and the original signal can be reconstructed from the wavelet transform. With the decrease of scale a, the support for the wavelet decreases and the wavelet transform becomes more sensitive to high-frequency components of the signal. The wavelet we used is the first derivative of a Gaussian smoothing function. The wavelet and the smoothing function are shown in Fig. 1.

The wavelet transform depends upon two parameters, scale a and position τ, which vary continuously over the real numbers. For smaller values of scale a, the wavelet is contracted in the time domain and the wavelet transform gives information about the finer details of the signal. For larger values of a, the wavelet expands and the wavelet transform gives a global view of the signal. The Fourier transform

 0739-5175/97/$10.00©1997

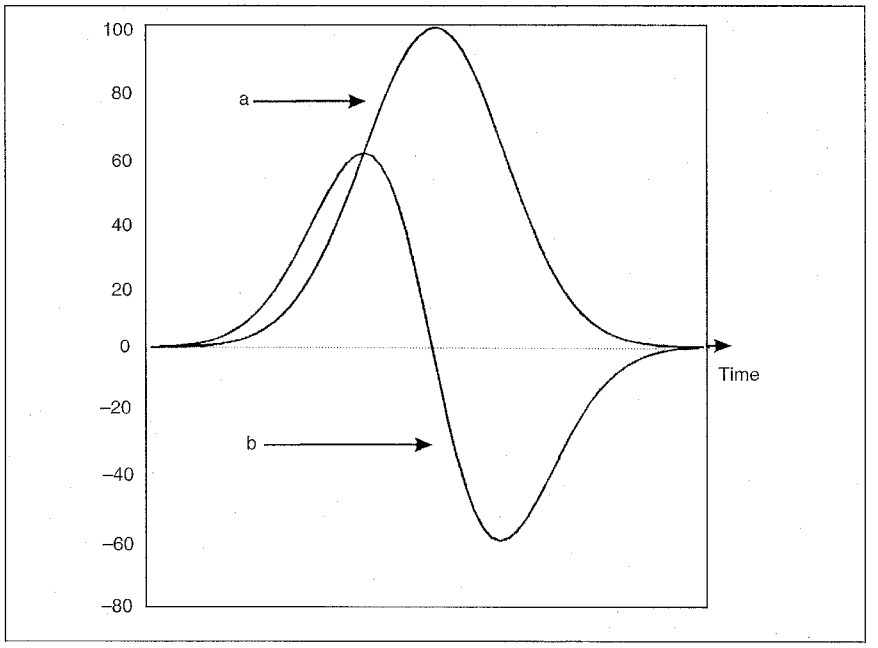

1. (a) Smoothing function and (b) the wavelet.

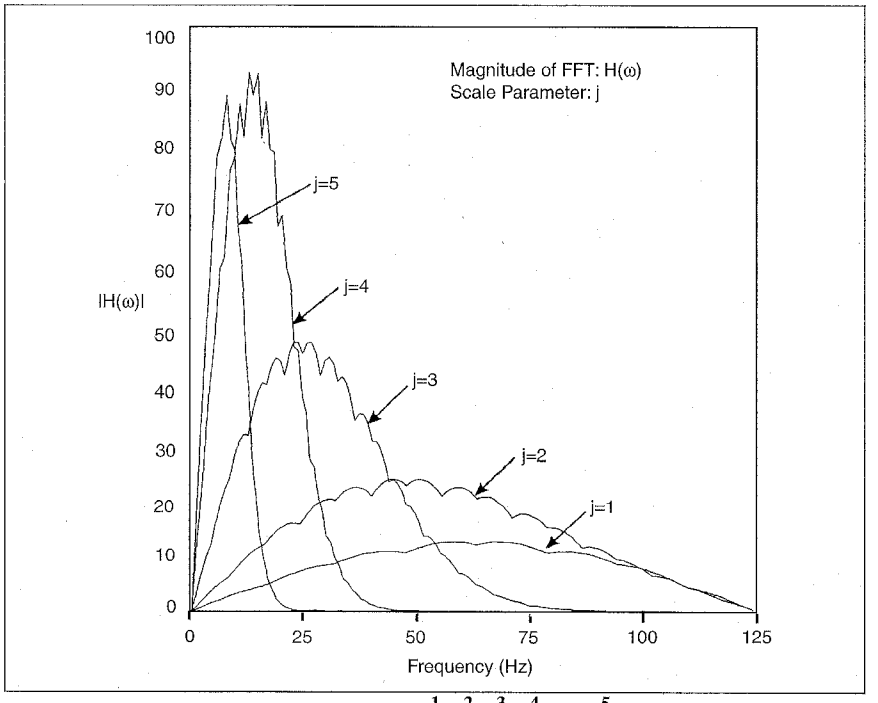

2. Fourier transform of wavelets at scale 2^1, 2^2, 2^3, 2^4 and 2^5. The ripples in the FFT are due to digital quantization of the wavelets.

of the wavelets at various scales is shown in Fig. 2. The wavelets pass bands are shown in Table 1. If the scale parameter is the set of integral powers of 2, i.e., $a = 2^j$ ($j \in Z$, Z is integer set), then the wavelet is called a dyadic wavelet [8].

The wavelet transform at scale 2^j is given by:

$$Wf(2^j,\tau) = \frac{1}{\sqrt{2^j}} \int_{-\infty}^{\infty} f(t) \Psi^* \left(\frac{t-\tau}{2^j} \right) dt \quad (5)$$

To cover the whole frequency domain, the Fourier transform of $\Psi_{2^j}(t)$ must satisfy the relation:

$$\sum_{j=-\infty}^{\infty} \left| \hat{\Psi}(2^j \omega) \right|^2 = 1 \quad (6)$$

Detection

QRS Complex

The detection of the QRS complex is based on modulus maxima of the wavelet transform, defined as any point $Wf(2^j,\tau_0)$ such that $|Wf(2^j,\tau)| < |Wf(2^j,\tau_0)|$ when τ belongs to either the left or right neighborhood of τ_0, and $|Wf(2^j,\tau)| \leq |Wf(2^j,\tau_0)|$ when τ belongs to the other side of the neighborhood of τ_0. This is because modulus maxima and zero crossings of the wavelet transform correspond to the sharp edges in the signal [9]. The QRS complex produces two modulus maxima with opposite signs of $Wf(2^j,\tau)$, with a zero crossing between them (Fig. 3). Therefore, it is determined by applying detection rules (thresholds) to the wavelet transform of the ECG signal.

Most of the energy of the QRS complex lies between 3 Hz and 40 Hz [11]. The 3-dB frequencies of the Fourier transform of the wavelets (Table 1) indicate that most of the energy of the QRS complex lies between scales of 2^3 and 2^4, with the largest at 2^4. The energy decreases if the scale is larger then 2^4. The energy of motion artifacts and baseline wander (i.e., noise) increases for scales greater then 2^5. Therefore, we chose to use characteristic scales of 2^1 to 2^4 for the wavelet.

The QRS complex corresponds to two modulus maxima with opposite signs of the wavelet transform (Fig. 3), i.e., a biphasic shape. The modulus maxima that correspond to the R-wave are determined by the following steps:

Step 1: The modulus maxima at the largest scale, 2^4, that cross threshold Th_4 are determined (Th_j is the threshold for wavelet transform at scale 2^j) and their positions $\{n_k^4 \mid k = 1..N\}$ are marked.

Step 2: The modulus maxima in the neighborhood of n_k^4 at scale 2^3 is determined and its location is marked as n_k^3. If several modulus maxima exist, then the largest one is selected. If no modulus maxima exist, then n_k^3, n_k^2, n_k^1 are set to zero.

Step 3: Similarly, the location set of modulus maxima $\{n_k^4, n_k^3, n_k^2, n_k^1 \mid k=0..N\}$ at remaining scales are determined.

In the above steps, the search for modulus maxima is made first at larger scales (i.e., 2^4) and then at finer scales (i.e., 2^3, 2^2, and 2^1). This strategy reduces the affect of high-frequency noise, which is present more in the lower scales, and also

there is a smaller number of modulus maxima in larger scales. Following this procedure, appropriate thresholds are applied to modulus maxima at the large scale to detect the modulus maxima corresponding to the QRS complex.

Usually, a given R-wave corresponds to a modulus maxima pair with opposite signs (i.e., a maxima and a minima) of wavelet transform. But in some ectopic beats or in the presence of noise, two or more modulus maxima can occur, of which only one is useful. If two negative minima MIN1 and MIN2 are near a positive maxima, with A1 and A2 as their absolute values, and L1 and L2 as their respective distances from the maxima, then the rule for judging which minima is extraneous is:

1. If A1/L1 > 1.2 A2/L2, MIN2 is redundant
2. If A2/L2 > 1.2 A1/L1, MIN1s is redundant
3. If MIN1 and MIN2 are on the same side of the maxima, then the minimum at the greater distance from the maxima is redundant. This is true even if the most-distant minima is larger than the peak of the closest minima, due to the fact that maxima and minima produced by rising and falling edge of the QRS complex will be adjacent. This same procedure can be applied to one negative minimum and two positive minima.

The R-wave corresponds to positive maxima and a negative minima pair at each scale, and the interval between two modulus maxima at scale 2^1 is slightly less than the QRS width. If this interval is greater than a certain time limit, then the modulus maxima is an isolated one and should be eliminated from the set of true modulus maxima. This interval should be less then the widest possible QRS complex (150 ms [11]). Here, the value of this interval is taken as 120 ms.

According to the relation of a signal and its wavelet transform, the zero crossings at scale 2^1 correspond to the R-peak. If all redundant and isolated modulus maxima are eliminated, then the remaining modulus maxima pairs correspond to the QRS complex. The thresholds used are Th_1, Th_2, Th_3, and Th_4, for scales 2^1, 2^2, 2^3, and 2^4, respectively. These thresholds adapt to the signal in order to track the signal variations. If a very sharp noise peak occurs, then the value of the peak modulus maxima will be large. In order to avoid errors, the parameter A_j^{m+1}(estimated modulus maxima for calculation of

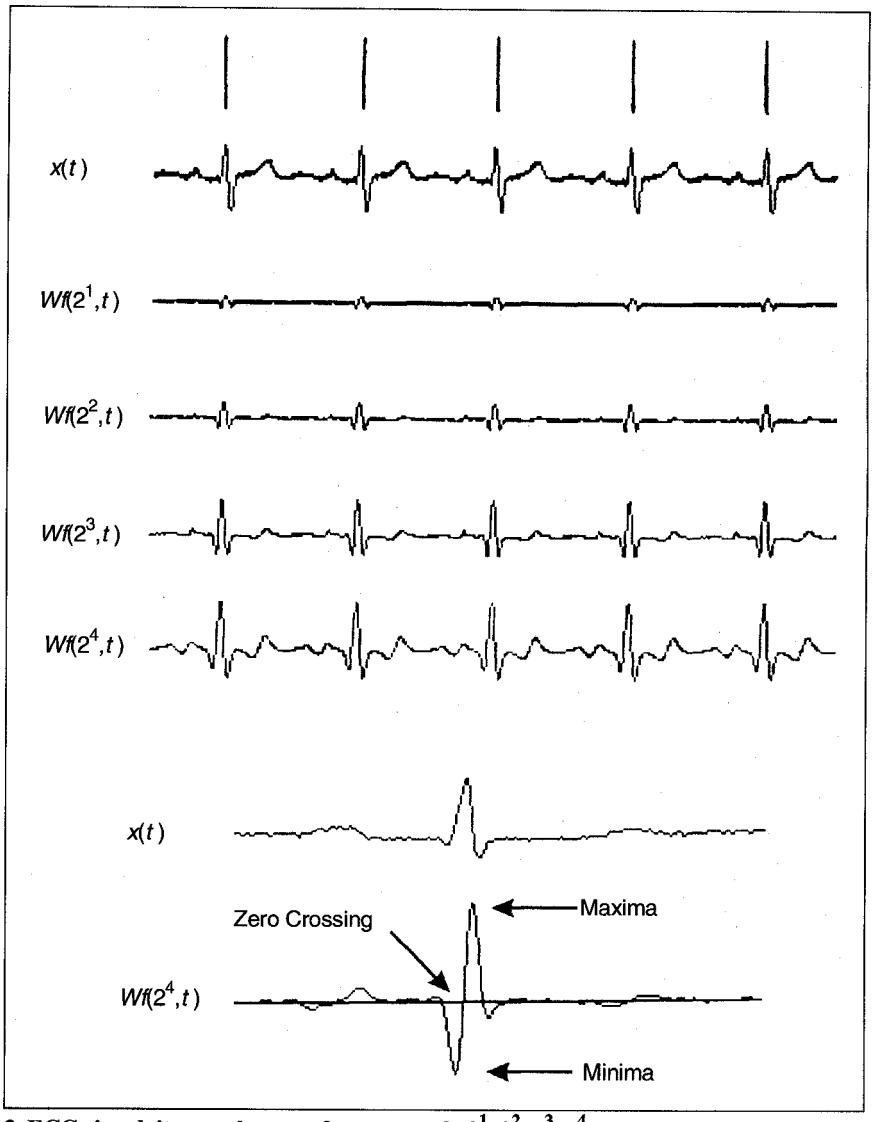

3. ECG signal, its wavelet transforms at scale 2^1, 2^2, 2^3, 2^4; maxima; minima; and zero crossing of wavelet transform at scale 24. The vertical lines above the ECG signal indicate the position of the QRS complex, as detected by the algorithm.

threshold for the next QRS complex) is kept the same (equal to the previous estimate, A_j^m) if the modulus maxima $|Wf(2^j,n_j^k)|$ is greater then twice the A_j^m.

If $|Wf(2^j,n_j^k)| \geq 2A_j^m$

then: $A_j^{m+1} = A_j^m$ (7)

otherwise:

$$A_j^{m+1} = \left(\frac{7}{8}\right)A_j^m + \left(\frac{1}{8}\right)|Wf(2^j,n_j^k)| \quad (8)$$

$Th_j = 0.3$, for $j = 1,2,3,4$

where Th_j is the threshold at scale 2^j.

To further improve the detection accuracy, the following standard precautions are observed:

1. As no two QRS complexes can occur in less then 200 ms [10], a 200 ms refractory period is used.

2. If a QRS complex is not found within a certain limit, then a search back is made with lower thresholds ($0.5Th_j$). During the forward search, the position of modulus maxima pairs, which cross either the full thresholds or the lower thresholds and satisfy the conditions for a QRS complex, are noted. During the search back, we already have the position of QRS complexes that have been missed by larger thresholds. Therefore, in search back, no extra processing time is required, and the system remains on-line.

Figure 3 shows the ECG waveform and the wavelet transform at various scales. The vertical lines above the ECG signal indicate the position of the QRS complex

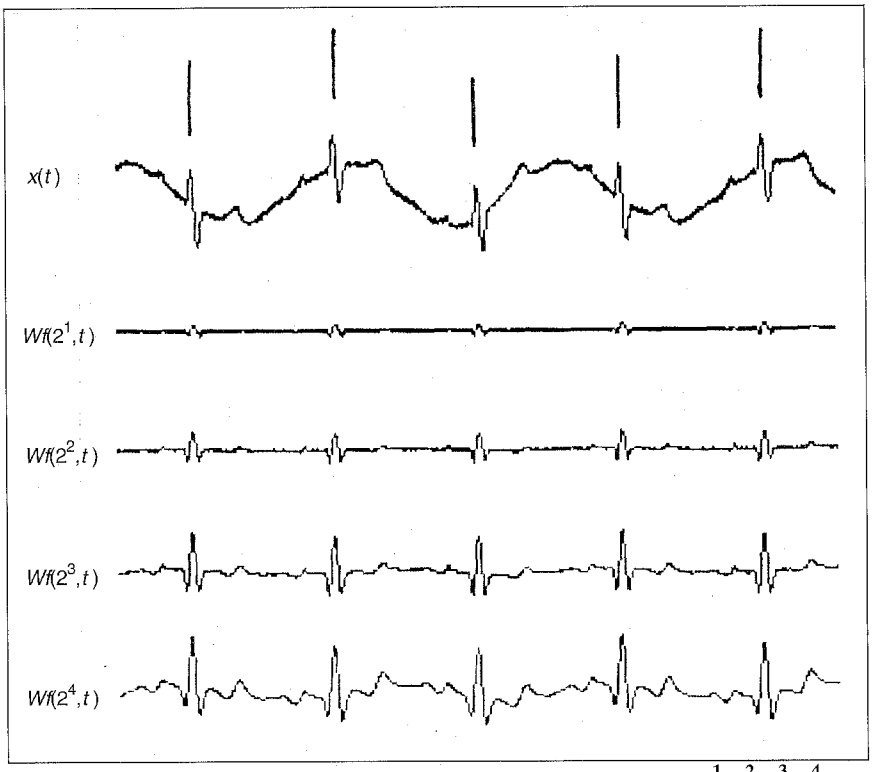

4. ECG signal with baseline drift and its wavelet transforms at scale 2^1, 2^2, 2^3, 2^4. The vertical lines above ECG signal indicate the position of the QRS complex, as detected by the algorithm.

Table 1. Frequency response of the wavelets at scales 2^1, 2^2, 2^3, 2^4, and 2^5.

Scale *a*	Lower 3 dB Frequency Hz	Upper 3 dB Frequency Hz
2^1	32.1	92.1
2^2	18.6	65.4
2^3	9.1	33.1
2^4	4.1	16.2
2^5	2.2	7.8

as detected by the algorithm. Figure 4 depicts the same thing, but with baseline drift, as does Fig. 5 but with 50 Hz interference.

Onset, Offset and Width of QRS complex

QRS width is calculated from the onset and offset of the QRS complex. The onset is the beginning of the Q-wave (or R-wave if the Q-wave is missing) and the offset is the ending of the S-wave (or R-wave if the S-wave is missing). Normally, the onset of the QRS complex contains the high-frequency components, which are detected at finer scales. The onset is the beginning and the offset is the ending of the first modulus maxima pair.

Onset, Offset, and Width of P and T Waves

The P- and the T-wave power spectra lie in the range of 0.5 Hz to 10 Hz [11], while baseline and motion artifacts have a frequency of 0.5 Hz to 7 Hz [11]. In order to avoid errors in detecting the onset and offset of these waves due to baseline drift and motion artifact, the 2^3 scale is selected.

The P-wave generally consists of a modulus maxima pair with opposite signs, and its onset and offset correspond to the onset and offset of this pair. This pair of modulus maxima is searched for within a window prior to the onset of the QRS complex. The search window starts at 200 ms before the onset of the QRS complex and ends with the onset of the QRS complex. The peak and width of the P-wave are found with the following steps:

1. The modulus maxima is a point where the $|Wf(2^3,\tau)|$ is at a maximum (the slope of $|Wf(2^3,\tau)|$ will equal zero).

2. The zero crossing between the modulus maxima pair corresponds to the peak of the P-wave.

3. To find the onset, a backward search is made from the point of modulus maxima that is on the left of the zero crossing, to the start of the search window, until a point is reached where the $|Wf(2^3,\tau)|$ becomes equal to or less then 5% of the modulus maximum. This point is marked as the onset of the P-wave. Empirically, it has been found that this 5% criteria best approximates the onset and offset of the P-and the T-waves.

4. To find the offset, a forward search is made from the point of modulus maxima that is on the right of the zero crossing, to the end of search window, until a point is reached where the $|Wf(2^3,\tau)|$ becomes equal to or less then 5% of the modulus maximum (modulus minimum). This point is marked as the offset of the P-wave.

The T-wave has characteristics similar to the P-wave. The detection procedure is the same as that for the P-wave, except that the search window follows the QRS complex. The T-wave onset is considered to be same as the offset of proceeding QRS complex.

PR Interval, ST Interval, and QT Interval

The PR interval is defined as the interval between the onset of the P-wave and the onset of the R-wave. The ST interval is the interval between the offset of the S-wave and offset of the T-wave. The QT interval is calculated by finding the difference between the onset of the Q-wave and the offset of T-wave. These definitions of timing intervals are shown in Fig. 6(a). Fig. 6(b) shows an example of measured values for one beat.

Implementation

Hardware

The system uses the Texas Instruments model TMS 320C25 DSP, which has an instruction time of 100 ns and is capable of performing 5 million instructions per second (MIPS). It has a modified Harvard

Table 2. Results of QRS detection of the system using the standard MIT BIH ECG database. The table gives the total number of times the detection failed (false positives and false negatives) and the accuracy of QRS detection.

ECG Record Name	Beats Analyzed for QRS Detection	False Positives (FP) (beats)	False Negatives (FN) (beats)	Detection Failed FP+FN (beats)	Accuracy of QRS Detection (%)
100	1901	0	0	0	100.00
101	1523	0	0	0	100.00
102	1816	0	0	0	100.00
103	1728	0	0	0	100.00
104	1852	1	0	1	99.95
105	2181	91	64	155	92.90
106	1696	1	10	11	99.44
107	1784	0	10	10	99.44
Total	14481	93	84	177	98.78

architecture, which allows it to access program and data simultaneously, increasing the speed of calculations. The instruction set is optimally designed for DSP applications, wavelets, and FFT. The processor also has a 4K x 16 bit on-chip masked ROM (for one-time programmablity). The DSP card is hosted inside the PC and communicates data and program with it through 8-bit ports.

Software

The various tasks done by the DSP card are as follows:

Data Acquisition

The ECG is sampled by a 16-bit Burr Brown bipolar analog-to-digital converter with a dynamic range of −10 to 10 and a resolution of 0.3 mv. The signal is sampled at 250 Hz.

Analysis

The wavelet transform of the signal is obtained using Eq. (5). Computation of the wavelet transform is restricted to the scales of interest, which are 2^1, 2^2, 2^3, and 2^4. The modulus maxima are found in all scales and their positions, and the magnitude of the wavelet transform is noted. The program then detects the modulus maxima that correspond to the QRS complexes. The zero crossing of the wavelet transform between the modulus maxima pairs corresponds to the R-point in the QRS complex. The QRS onset and offset are determined as described above. A similar procedure is carried out for localization of the P- and the T-waves to calculate their onsets and offsets. Once the onset and offset of the P-, the QRS- and the T-waves are known, the PR interval, ST interval, and QT intervals are calculated (Fig. 6(b)). Hence, the time characterization of the ECG is accomplished.

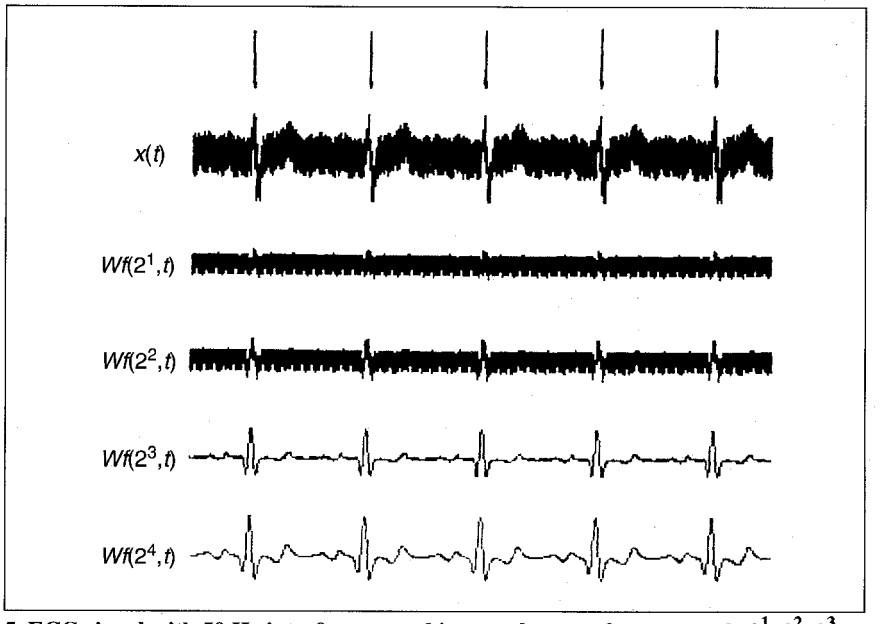

5. ECG signal with 50 Hz interference and its wavelet transforms at scale 2^1, 2^2, 2^3, 2^4. The vertical lines above ECG signal indicate the position of the QRS complex, as detected by the algorithm.

Results

Eight ECG data files, each of 30 min duration from the MIT BIH ECG database, were used to evaluate QRS detection. Channel 1 of the ECG data files was used as input to the system. The results of the QRS detection are given in Table 2. As given in the database manuals, the first five minutes of data of each record is taken as the learning period, and comparison starts after that. Record 105 shows 64 false positives and 91 false negatives (out of a total of 2181 beats). This is because of heavy motion artifact. Overall the system shows the accuracy of 98.8%.

For the evaluation of system performance for detection of onset and offsets of the P, QRS, and the T complexes, the standard CSE ECG library was used. In Table 3, the results are given in the form of standard deviation (SD) of the differences between the calculated values of onsets (and offsets) and the final referee estimates (median) of the CSE Committee. The corresponding acceptable limits of SD recommended by the CSE committee are also given in the table [12]. The

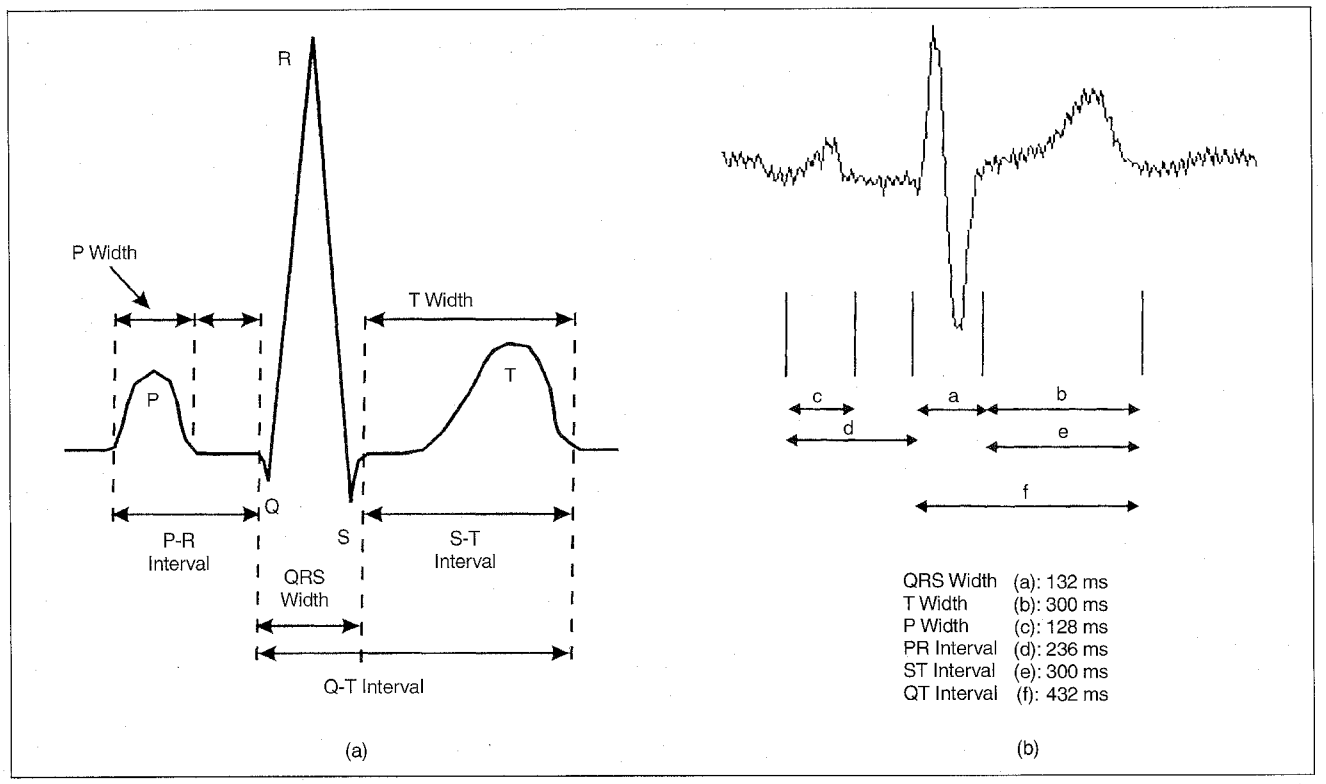

6. (a) Definition of timing intervals of the QRS complex. (b) Measured values of timing intervals of one QRS complex.

Table 3. Results for the accuracy of detection of onsets and offset of the P, the QRS and the T end with the standard CSE ECG Database. The standard deviation of the differences between the calculated value and the final referee estimate (median) are given along with the limit of SD recommended by the CSE committee. The SD is well within the acceptable limits.

	Standard Deviation (ms)	Limit of Standard Deviation (ms) (By CSE committee)
P onset	4.0	10.2
P offset	6.0	12.7
QRS onset	2.0	6.5
QRS offset	4.0	11.6
T end	20.0	32.5

results show that the SD is within the acceptable limits.

Conclusions

On-line digital signal processing using multiresolution analysis (wavelet transforms) has been described to provide precise information of timing intervals that define the morphology of the ECG. Noise generally encountered in the clinical environment is automatically eliminated due to inherent characteristics of the technique. The accuracy of the system & technique has been validated using the MIT BIH ECG database and the Standard CSE ECG library.

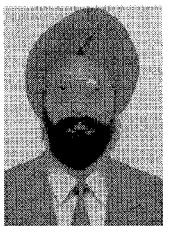

J.S. Sahambi graduated in in 1989 with a degree in Electrical Engineering from Guru Nanak Engineering College, Ludhiana, Punjab (Punjab University),. He obtained his M. Tech. degree in Computer Technology from I.I.T. Delhi in 1991. He is a faculty member of the Microprocessor Application Programme under the Electrical Engineering department at I.I.T. Delhi. At present he is working for his Ph.D. degree in the Center for Biomedical Engineering, I.I.T. Delhi. His current research interests include digital signal processing, microprocessor applications, and biosignal processing.

S.N. Tandon received his B.E. and M.E. degrees in Electronics Engineering from Roorkee University in 1965 and 1968, respectively. He obtained his Ph.D. degree from I.I.T. Delhi in Biomedical Engineering. He worked in the Biomedical Engineering unit on a collaborative program between MIT and Harvard Medical School, USA, from 1969-71. He has been a faculty member of I.I.T. Delhi since 1971. Currently he is a professor in Center for Biomedical Engineering, I.I.T. Delhi. His current research interests are biosignal processing, medical imaging, and microprocessor applications in medicine.

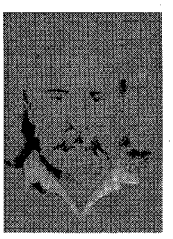

R.K.P. Bhatt received his B.E. degree from Ravishankar University, Raipur, in 1969. He received his M. Tech degree from I.I.T. Kanpur in 1971 and Ph.D. in 1981 from I.I.T. Delhi. Currently he is an Assistant Professor in the Electrical Engineer-

ing Department at I.I.T. Delhi. His research interests include signal & image processing, adaptive control, and neural networks.

Address for Correspondence: Prof. S.N. Tandon, Centre for Biomedical Engineering, Indian Institute of Technology, Delhi Hauz Khas, New Delhi PIN 110016, India.

References

1. **Tompkins WJ, Pan J:** A real time QRS detection algorithm, *IEEE Transactions on Biomedical Engg.* BME-32, No. 3:230-235, March 1985.

2. **Coast DA, Stern RM, Cano GG, Briller SA:** An approach to cardiac arrhythmia analysis using hidden Markov models, *IEEE Transactions on Biomedical Engg.* Vol. 37, NO. 9:826-836, September 1990.

3. **Kyrkos A, Giakoumakis EA, Carayannis G:** QRS Detection through time recursive prediction techniques, *Signal Processing* 15:429-436, 1988.

4. **Daubechies I:** The wavelet transform: A method of time frequency localization, In: *Advances in Spectral Analysis.* S Haykin, Ed. New York, Prentice Hall, 1990.

5. **Mallat S:** Multiresolution frequency channel decomposition of images and wavelet models: *IEEE Transactions on Acoust, Speech Signal Processing*, 37, No. 12: 2091-2110, 1989.

6. **Rioul O,Vetterli M:** Wavelet and signal processing, *IEEE Signal Processing Magazine*:14-38, Oct. 1991.

7. **Chui K.:** *An Introduction to Wavelets*, Academic Press, Inc.1992

8. **Mallat S:** Zero crossings of wavelet transform, *IEEE Trans. Information Theory*, 37, No. 4, 1019-1033, July 1991.

9. **Cuiwei L, Chongxum Z, Changfeng T:** Detection of ECG Characteristic Points Using Wavelet Transforms, *IEEE Transactions on Biomedical Eng.*, 42. No. 1: 22-28,January 1995.

10. **Hamilton PS, Tompkins WJ:** Quantitative Investigation of QRS Detection Rules Using MIT BIH Arrhythmia Database, IEE Transactions on Biomedical Engg. Vol. BME-33, No. 12, Dec 1986.

11. **Thakor NV, Webstor JG, Tompkins WJ:** Estimation of QRS Complex Power Spectra for Design of a QRS Filter, *IEEE Trans. Biomedical Engg.*, Vol. BME-31, No.11: 702-705, 1984.

12. **The CSE Working Party:** Recommendations for Measurement of Standards in Quantitative Electrocardiography, *Eur. Heart J.* 6, 815, (1985).

Errata

■ Please note the following corrections to the article titled "Reducing Correlated Noise in Digital Hearing Aids," which appeared in the September/October issue of *Engineering in Medicine and Biology Magazine*:

On page 91 in the second line of column 1, $p_{\hat{N}}\left(\tilde{\mathbf{n}};\mathbf{R}_{\tilde{N}}\right)$ should have read $p_{N|\tilde{N}}\left(\mathbf{n}|\tilde{\mathbf{n}};\mathbf{R}_{N}\right)$.

Also on page 91, Eq. 10 should have read:

$$L\left(\mathbf{x},\lambda^{(k)}\right)\approx\frac{1}{2\sigma_u^2\ln 2}\sum_{\ell=p}^{N-1}\left(\sum_{m=0}^{N-1}\alpha_m n_{\ell-m}\right)^2+C_3$$

On page 92, Eq. 25 and text that follows it should have read:

$$\left|\lambda_x(j,k,m)\right|\geq\frac{\sigma_u\sqrt{3\ln N}}{\frac{1}{2^{-j}N}\sum_{m'=0}^{2^{-j}N-1}\left\|\mathbf{A}^{\mathrm{H}}\phi(j,k,m')\right\|}$$

for $m\in\left\{0,1,\ldots 2^{-j}N-1\right\}$. Hence...

On page 96, the publication date for Reference 21 should be 1993, not 1995.

We and the authors regret any inconvenience these errors may have caused.

■ In the November/December 1996 issue of *Engineering in Medicine and Biology Magazine*, on page 112 of the article titled "Using Biofeedback for Standing-Steadiness, Weight-Bearing Training," the affiliation of author M.Y. Lee was incorrectly listed as Chang Gung Memorial Hospital. His correct affiliation is the Chang Gung College of Medicine and Technology's Mechanical Engineering Department. We apologize to the author and our readers for this error.